

1 **Supplementary methods**

3 **Cell lines**

4 Human cell lines were grown at 37°C, 5% CO₂. a) Human myeloma (HM)-CLs: AMO1, NCI-
5 H929, SK-MM-1, U266, JJN3 and KMS-12-BM were purchased from DSMZ (Braunschweig,
6 Germany). MM.1S, MM.1R and RPMI-8226 were purchased from ATCC (Manassas, VA,
7 USA). AMO1 bortezomib-resistant (ABZB) and AMO1 carfilzomib-resistant (ACFZ) were
8 kindly provided by Dr. Christoph Driessen (Eberhard Karls University, Tübingen, Germany).
9 U266 melphalan-resistant (LR7) were kindly provided by Dr. Atanasio Pandiella
10 (Universidad de Salamanca, Salamanca, Spain). KMS-11 were kindly provided by Dr. K.C.
11 Anderson (Dana-Farber Cancer Institute, Harvard Medical School, Boston, MA, USA). KMS-
12 26 were kindly provided by Dr. Giovanni Tonon (University of San Raffaele Scientific
13 Institute, Milan, Italy). These cells were cultured in RPMI-1640 medium (Gibco® Life
14 Technologies, Carlsbad, CA, USA) supplemented with 10% fetal bovine serum (Lonza
15 Group Ltd., Basel, Switzerland) and 1% penicillin/streptomycin (Gibco®, Life Technologies).
16 IL-6 dependent cell lines INA-6 and XG-1, kindly provided by Dr. Renate Burger (University
17 of Erlangen-Nuernberg, Erlangen, Germany), were cultured in the presence of 1 ng/mL rhIL-
18 6 (R&D Systems, Minneapolis, MN). b) Mantle cell lymphoma (MCL)-CLs: Mino, Maver-1
19 and Jeko-1 (purchased from ATCC) were cultured in RPMI-1640 medium (Gibco® Life
20 Technologies) supplemented with 10% fetal bovine serum (Lonza Group Ltd.) and 1%
21 penicillin/streptomycin (Gibco®, Life Technologies). c) Diffuse large B cell lymphoma
22 (DLBCL)-CLs: Oci-Ly-7, Pfeiffer and Toledo (purchased from ATCC) were cultured in RPMI-
23 1640 medium (Gibco® Life Technologies) supplemented with 10% fetal bovine serum
24 (Lonza Group Ltd.) and 1% penicillin/streptomycin (Gibco®, Life Technologies). d) Burkitt
25 lymphoma (BL)-CLs: Sultan, P3HR1, Daudi and Raji (purchased from ATCC) were cultured
26 in RPMI-1640 medium (Gibco® Life Technologies) supplemented with 10% fetal bovine
27 serum (Lonza Group Ltd.) and 1% penicillin/streptomycin (Gibco®, Life Technologies). e) T
28 cell lymphoma (TCL)-CLs: H9 and Jurkatt (purchased from ATCC) were cultured in RPMI-
29 1640 medium (Gibco® Life Technologies) supplemented with 10% fetal bovine serum
30 (Lonza Group Ltd.) and 1% penicillin/streptomycin (Gibco®, Life Technologies). f) Acute
31 myeloid leukemia (AML)-CLs: THP-1, K562, HL-60 (purchased from ATCC) were cultured
32 in RPMI-1640 medium (Gibco® Life Technologies) supplemented with 10% fetal bovine
33 serum (Lonza Group Ltd.) and 1% penicillin/streptomycin (Gibco®, Life Technologies). g)
34 Malignant pleural mesothelioma (MPM)-CLs: Mero-14, Mero-25, MPM-209, MPM-376 and
35 IST-MES (kindly provided by Department of Pharmaceutical Sciences, University of

36 "Piemonte Orientale Amedeo Avogadro", Novara, Italy) were cultured in DMEM (Dulbecco's
37 modified Eagle's medium) (Gibco®, Life Technologies) supplemented with 10% fetal bovine
38 serum (Lonza Group Ltd.) and 1% penicillin/streptomycin (Gibco®, Life Technologies). h)
39 Pancreatic cancer (PC)-CLs: Capan-1 and BxPC-3 (purchased from Istituto Zooprofilattico
40 Sperimentale della Lombardia e dell'Emilia Romagna (IZLER), Brescia, Italy) were cultured
41 in RPMI-1640 medium (Gibco®, Life Technologies) supplemented with 20% fetal bovine
42 serum (Lonza Group Ltd.) and 1% penicillin/streptomycin (Gibco®, Life Technologies);
43 Capan-2, AsPC-1, PANC-1 and MIA PaCa-2 (purchased from ATCC) were cultured in
44 DMEM (Dulbecco's modified Eagle's medium) (Gibco®, Life Technologies) supplemented
45 with 10% fetal bovine serum (Lonza Group Ltd.) and 1% penicillin/streptomycin (Gibco®,
46 Life Technologies). i) Breast cancer (BC)-CLs: MCF7 (purchased from ATCC) were cultured
47 in ATCC-formulated Eagle's Minimum Essential Medium, supplemented with 0.01 mg/ml
48 human recombinant insulin, 10% fetal bovine serum (Lonza Group Ltd.) and 1%
49 penicillin/streptomycin (Gibco®, Life Technologies); MDA-231 (purchased from ATCC) were
50 cultured in ATCC-formulated Leibovitz's L-15 Medium, supplemented with 10% fetal bovine
51 serum (Lonza Group Ltd.) and 1% penicillin/streptomycin (Gibco®, Life Technologies);
52 HCC1937 (purchased from ATCC) were cultured ATCC-formulated Leibovitz's L-15 Medium,
53 supplemented with 15% fetal bovine serum (Lonza Group Ltd.) and 1%
54 penicillin/streptomycin (Gibco®, Life Technologies); SK-BR-3 (purchased from ATCC) were
55 cultured in RPMI-1640 medium (Gibco®, Life Technologies) supplemented with 10% fetal
56 bovine serum (Lonza Group Ltd.) and 1% penicillin/streptomycin (Gibco®, Life
57 Technologies). j) Non-small cell lung cancer (NSCLC)-CLs: A-549, LXF-289 (purchased
58 from ATCC) were cultured in RPMI-1640 medium (Gibco®, Life Technologies)
59 supplemented with 10% fetal bovine serum (Lonza Group Ltd.) and 1%
60 penicillin/streptomycin (Gibco®, Life Technologies). k) Non-malignant (NM)-CLs: 293T
61 (human embryonic kidney) and HS-5 (human stromal cells) were purchased from ATCC and
62 cultured in DMEM (Dulbecco's modified Eagle's medium) (Gibco®, Life Technologies)
63 supplemented with 10% fetal bovine serum (Lonza Group Ltd.) and 1%
64 penicillin/streptomycin (Gibco®, Life Technologies); HK-2 (human kidney cells,
65 cortex/proximal tubule) were purchased from ATCC and cultured in K-SFM (Keratinocyte
66 Serum Free Medium) (Thermo Fisher Scientific, Waltham, MA, USA). supplemented in
67 accordance with ATCC guide lines; THLE-2 (human liver cells) were purchased from ATCC
68 and cultured in BEGM (Bronchial epithelial cell growth medium) (Lonza Group Ltd.)
69 supplemented in accordance with ATCC guide lines; HCC-1143-B1 (human B cells) were

70 purchased from ATCC and cultured in RPMI-1640 medium (Gibco® Life Technologies)
71 supplemented with 10% fetal bovine serum (Lonza Group Ltd.) and 1%
72 penicillin/streptomycin (Gibco®, Life Technologies). l) P493-6 were kindly provided by Dr.
73 Dirk Eick (Max Planck Institute of Biochemistry, Helmholtz-Zentrum München, Germany and
74 cultured in RPMI-1640 medium (Gibco® Life Technologies) supplemented with 10% fetal
75 bovine serum (Lonza Group Ltd.) and 1% penicillin/streptomycin (Gibco®, Life
76 Technologies). m) MYC-ER HMEC were kindly provided by Dr. Stephen J. Elledge (Howard
77 Hughes Medical Institute, Harvard Medical School, Brigham & Women's Hospital, Boston,
78 MA02115, USA) and cultured in MEGM (Mammary Epithelial Cell Growth Medium) (Lonza
79 Group Ltd.) supplemented according to manufacturer's instructions.
80 Cells were periodically tested to exclude mycoplasma contamination. Cells were STR (short
81 tandem repeats) authenticated.

82

83 **Primary patient cells**

84 Following informed consent approved by our University Hospital Ethical Committee,
85 CD138+ cells were isolated from the BM aspirates of both MGUS and MM patients by Ficoll-
86 Hypaque (Lonza Group, Basel, Switzerland) density gradient sedimentation, followed by
87 antibody-mediated positive selection using anti-CD138 magnetic activated cell separation
88 microbeads (Miltenyi Biotech, Gladbach, Germany). Purity of immunoselected cells was
89 assessed by flow-cytometry analysis using a phycoerythrin-conjugated CD138 monoclonal
90 antibody by standard procedures. For co-culture experiments: CD138+ cells from MGUS
91 patients and from MM patients pt#1, pt#2 and pt#3 were seeded on HS-5 cells and cultured
92 in RPMI-1640 medium (Gibco®, Life Technologies) supplemented with 10% fetal bovine
93 serum (Lonza Group Ltd.) and 1% penicillin/streptomycin (Gibco®, Life Technologies);
94 CD138+ cells from MM patients pt#4, pt#5, pt#6, pt#7, pt#8, pt#9, pt#10 and pt#11 were
95 cultured physically separated from HS-5 cells by means of Falcon Cell Culture Inserts
96 (Corning, New York, NY, USA), according to manufacturer's instructions. CD138+ cells from
97 MM patients pt#12 and pt#13 were cultured in RPMI-1640 medium (Gibco®, Life
98 Technologies, Carlsbad, CA, USA) supplemented with 10% fetal bovine serum (Lonza
99 Group Ltd., Basel, Switzerland) and 1% penicillin/streptomycin (Gibco®, Life Technologies).
100 Co-culture of HMCLs with hBMSCs was performed as previously reported¹⁰.

101

102 **Peripheral blood mononuclear cells**

103 Peripheral blood mononuclear cells (PBMCs) were isolated from healthy adult donors, after
 104 informed consent approved by our University Hospital Ethical Committee. Cells were
 105 separated using Ficoll-hypaque method (Lonza Group Ltd.). PBMCs were cultured in RPMI-
 106 1640 medium (Gibco®, Life Technologies) supplemented with 10% fetal bovine serum
 107 (Lonza Group Ltd.) and 1% penicillin/streptomycin (Gibco®, Life Technologies).

108

109 **Antisense oligonucleotides, miRNA mimics/inhibitors and shRNAs**

110 The following Long Non-Coding LNA gapmerRs were customly-designed and purchased
 111 from Exiqon (Vedbaek, Denmark):

112

113

IDS, Sequence and length of seven miR-17-92 LNA gapmeRs and three controls.

IDS	SEQUENCE 5'-3'	LENGHT (mer)
LNA gapmeR_02	ACATCGACACAATAA	15
LNA gapmeR_05	TCAGTAACAGGACAGT	16
LNA gapmeR_06 (MIR17PTi)	TACTTGCTTGGCTT	14
LNA gapmeR_10	ATGCAAAACTAACAGA	16
LNA gapmeR_12	GAAGGAAAATAGCAGGC	16
LNA gapmeR_15	AGCACTCAACATCAGC	16
LNA gapmeR_16	CGACAGGCCGAAGCT	15
Scr-NC (also known as Negative control A)	AACACGTCTATACGC	15
Lp-MIR17PTi	TACTTGCTTGGCTT	14
mix-MIR17PTi	TACTTGCTTGGCTT	14

114

115 Synthetic mimics and inhibitors for miR-17a, miR-18a, miR-19a, miR-20a, miR-19b-1 and
 116 miR-92a1 were purchased from Ambion (Applied Biosystems, CA, US).

117 The following MIR17HG shRNAs (Mission 3x Lac0 IPTG Inducible shRNAs) were customly-
 118 designed and purchased from Sigma-Aldrich (Saint-Louis, Missouri, USA):

119 - *MIR17HG* shRNAs#1: tgggcttgaactgagatttaa

120 - *MIR17HG* shRNAs#2: tccaggcttatttgacttaaa

121 - *MIR17HG* shRNAs#3: tgggtgataaagtagatataa

122 A negative control (IPTG-inducible Non-targeting shRNAs) and a positive control (IPTG
 123 inducible TurboGFP shRNA) were also purchased from Sigma-Aldrich.

124 The following MIR17HG siRNAs (Lincode SMARTpool siRNA) were purchased from
 125 Dharmacon (Lafayette, Colorado):

126 - GCUUAGUGGGUAUGAGU (N-032556-09)

127 - CCGAAGAUGGUGGCGGCUA (N-032556-10)

128 - CACUUGAGACUUCAGAUUA (N-032556-11)

129 - GGCCUCCGGUCGUAGUAAA (N-032556-12)

130

131 **Transient transfection of cells**

132 Adherent cell lines: cells were transfected by Lipofectamine 2000 according to manufacturer
133 instructions with 25 nM of LNA gapmeRs (Exiqon).

134 Suspension cell lines: cells were transfected (electroporation) by Neon Transfection System
135 (Invitrogen, CA, US), (2 pulses at 1150, 30ms). LNA gapmeRs and miRNA inhibitors/mimics
136 were used at 25nM. MIR17HG pooled siRNAs were used at 500nM. The transfection
137 efficiency evaluated by flow-cytometric analysis relative to a FAM dye-labeled anti-miR-
138 negative control reached 85% to 90%.

139

140 **Transduction of cells**

141 To generate cells stably expressing luciferase transgene, U266, AMO-1 and AMO-1/abzb
142 cells were transduced with pLenti-III-PGK-Luc (ABM Inc., Richmond, BC, Canada) vector,
143 following the manufacturer's instructions. To generate cells stably over-expressing miR-17-
144 92 cluster, U266 were transduced with PMIRH17-92PA-1 lenti-vector (System Biosciences,
145 Palo Alto, CA, USA). To generate cells stably expressing c-MYC, U266 were transduced
146 with Precision LentiORF human MYC (GE Dharmacon, Lafayette, Colorado, USA).

147

148 **CRISPR/CAS9-mediated genome editing**

149 Genomic knock-out of BIM was achieved by transfection of AMO1 or U266^{MYC+} with
150 CRISPR/CAS9 all-in-one vectors (pCLIP-ALL-hCMV-ZsGreen) (transOMIC technologies
151 Inc., Huntsville, AL, USA). After two days, ZsGreen+ cells were sorted (BD FACSAria III;
152 BD Biosciences, Qume Drive San Jose, CA, USA) and single-cell cultured by limiting-dilution
153 technique. Single-cell derived clones (two for each vector, TEVH-1110175 / TEVH-1177317
154 / TEVH-1244459) were selected and used for downstream experiments.

155

156 **Gymnosis**

157 Cells were seeded at low plating density in order to reach confluence on the final day of the
158 experiments (day 6). Cell number at plating ranged from 0,5 to 2,5 x 10³ in 96-well plates,
159 from 2,5 to 10 x 10⁴ in 12-well plates and from 1 to 3 x 10⁵ in 6-well plates.

160

161 **Survival assay**

162 Cell viability was evaluated by Cell Counting Kit-8 (CCK-8) assay (Dojindo Molecular
163 Technologies) and 7-AminoactinoMYCin (7-AAD) flow cytometry assays (BD biosciences),
164 according to manufacturer's instructions. Flow cytometry analysis was performed either by
165 FACS CANTO II (BD biosciences) or by Attune NxT Flow cytometer (Thermo Fisher
166 Scientific).

167

168 **Detection of apoptosis**

169 Apoptosis was investigated by Annexin V/7-AAD flow cytometry assay (BD biosciences) and
170 by electronic microscopy. Flow cytometry analysis was performed either by FACS CANTO
171 II (BD biosciences) or by Attune NxT Flow cytometer (Thermo Fisher Scientific).

172

173 **Cell cycle analysis**

174 Analysis of cell cycle was performed by Propidium Iodide flow cytometry assay (BD
175 biosciences), according to manufacturer's instructions. Flow cytometry analysis was
176 performed either by FACS CANTO II (BD biosciences) or by Attune NxT Flow cytometer
177 (Thermo Fisher Scientific).

178

179 **Synergism quantification**

180 Drug combination studies and their synergy quantification followed the Chou-Talalay
181 method⁴⁰. First, dose-effect curves were determined in AMO1 after six days of treatment for
182 each drug, including dexamethasone, melphalan or bortezomib (Selleckchem.com). Then,
183 different concentrations of each anti-MM agent were combined to MIR17PTi ranging 0.75-
184 1.25 μ M. Combination indexes (CI) were calculated by CalcuSyn (BIOSOFT, Cambridge,
185 UK).

186

187 **Reverse transcription (RT) and quantitative real-time amplification (qRT-PCR)**

188 RNA extraction, reverse transcription (RT) and quantitative real-time amplification (qRT-
189 PCR) were performed as previously described¹⁰. Briefly, total RNA was extracted from cells
190 with TRIzol® Reagent (Thermo Fisher Scientific), according to manufacturer's instructions.
191 The integrity of total RNA was verified by nanodrop (Celbio Nanodrop Spectrophotometer
192 nd-1000). For pri-mir-17-92 and mRNA dosage studies, oligo-dT-primed cDNA was obtained
193 through the High Capacity cDNA Reverse Transcription Kit (Thermo Fisher Scientific) and
194 then used as a template to quantify has-pri-mir-17-92 (pri-mir-17: Hs03295901; pri-mir-92a-
195 1: Hs03302603), BIM (Hs00708019_s1), BZW2 (Hs00204063_m1), DUSP2

196 (Hs01091226_g1), CCNG2 (Hs00171119_m1), NAP1L1 (Hs00748775_s1), STAT3
197 (Hs00374280_m1), VDAC1 (Hs01631624_gH) and ARRDC3 (Hs00385845_m1). In all qRT-
198 PCR experiments both taqman probes for pri-mir-17-92 were used, but only results with pri-
199 mir-17 probe are shown. Normalization was performed with human GAPDH
200 (Hs03929097_g1). Single-tube TaqMan miRNA assay (Thermo Fisher Scientific) was used
201 to detect and quantify miR-17 (002308), miR-18a (002422), miR-19a (000395), miR-20a
202 (000580), miR-19b (000396) and miR-92a-1 (000431), according to the manufacturer's
203 instructions, by the use of ViiA7 RT reader (Thermo Fisher Scientific). Mature miRNAs
204 expression was normalized on RNU44 (Thermo Fisher Scientific, assay Id:
205 Hs03929097_g1). lncRNA MIR17HG-201 was detected by SYBR Green qRT-PCR using the
206 following primers: Fw, 5' CTGCCTTGATAACATTTTCATATGTGG; Rev, 5'
207 CTTCCGGCTCGTATGTTGTGTGG.

208 Comparative real-time polymerase chain-reaction (RT-PCR) was performed in triplicate,
209 including no-template controls. Relative expression was calculated using the comparative
210 cross threshold (Ct) method.

211

212 **Western blot analysis**

213 Protein extraction and western blot analysis were performed as previously described¹⁰.
214 Briefly, cells were lysed in lysis buffer containing 15mM Tris/HCl pH 7.5, 120mM NaCl, 25mM
215 KCl, 1mM EDTA, 0.5% Triton 100, Halt Protease Inhibitor Single-Use cocktail (100X,
216 Thermo Scientific). Whole cells lysates (~20 µg per lane) were separated using 4-12%
217 Novex Bis-Tris SDS-acrylamide gels (Invitrogen), electro-transferred on Nitrocellulose
218 membranes (Bio-Rad). After electrophoresis the nitrocellulose membranes were blocked
219 and probed over-night with primary antibodies at 4 °C, then the membranes were washed 3
220 times in PBS-Tween and then incubated with a secondary antibody conjugated with
221 horseradish peroxidase for 2 hours at room temperature. Chemiluminescence was detected
222 using Western Blotting Luminol Reagent (sc-2048, Santa Cruz, Dallas, TX, USA). Signal
223 intensity was quantified with the Quantity One Analyzing System (Bio-Rad).

224 Primary antibodies: BIM (#2933), Apaf-1 (#5088), Caspase 8 (#9746), Caspase-3 (#9665),
225 Stat3 (#4904) were purchased from Cell Signalling Biotechnology. CCNG2 (ab54901) and
226 BZW2 (ab96682) were purchased from Abcam (Cambridge, UK). GAPDH (sc-25778) and
227 β-actin (ab96682) were purchased from Santa Cruz Biotechnology (Dallas, TX, USA).

228

229 **Confocal Microscopy**

230 293T cells were treated with FAM-labeled MIR17PTi (2,5µM). After treatment, cells were
231 washed with PBS1X, centrifuged onto glass slides, fixed in 4% paraformaldehyde in PBS
232 for 12 minutes, and washed in PBS (3 times x 5 minutes). Cells were permeabilized (0,1 %
233 Triton X-100 in PBS) for 15 minutes, washed in PBS (3 times x 5 minutes), and incubated
234 for 1 hour with blocking buffer (1,5 % BSA in PBS). Cells were washed in PBS (3 times x 5
235 minutes) and mounted under coverslips with Prolong Antifade plus DAPI. Images were
236 acquired at confocal microscopy TCS SP II Leica Microsystems.

237

238 **Gene expression profiling**

239 Gene expression profiles were obtained from pMM cells (pt#5, pt#6, pt#7, pt#9) and AMO1
240 after six days of gymnotic exposure to MIR17PTi or scr-NC. Cells were collected and used
241 for total RNA (tRNA) extraction by RNeasy Mini kit (Qiagen, Hilden, Germany). A total of
242 300 ng RNA was used as starting material for preparing the hybridization target by using the
243 GeneChip® WT PLUS Reagent Kit (Affymetrix Inc., Santa Clara, CA, USA). The integrity,
244 quality and quantity of tRNA were assessed by the Agilent Bioanalyzer 2100 (Agilent
245 Technologies, Santa Clara, CA, USA) and NanoDrop 1000 Spectrophotometer (Thermo
246 Scientific, Wilmington, DE). The amplification of cRNA, the clean-up and the fragmentation
247 were performed according to the Affymetrix's procedures. Microarray data was generated
248 by GeneChip® Human Transcriptome 2.0 Array (Affymetrix Inc., Santa Clara, Ca). Arrays
249 were scanned with an Affymetrix GeneChip Scanner 3000. Raw data produced by the
250 Affymetrix Platform (i.e. CEL files) were first processed using Affymetrix Expression Console
251 (EC). Pre-processing phase was performed according to Affymetrix guidelines and micro-
252 CS software. Raw data were normalized using probe logarithmic intensity error (PLIER)
253 algorithm coupled to quantile normalization. Annotation of data was also performed using
254 Affymetrix Provided Libraries and EC version 1.4.1. Differential expression was assessed
255 using a linear model method. *P*-values were adjusted for multiple testing using the Benjamini
256 and Hochberg method. Tests were considered to be significant for adjusted *P*<0.05.
257 Clustering and fold change (FC) analysis were done using the dChip software comparing
258 relative gene expression of MIR17PTi *versus* scr-NC treated cells. For each pair of
259 compared samples we calculated FC as follows: $FC = \log_2(\text{MIR17PTi } \textit{versus} \text{ scr-NC})$. The
260 gene lists were applied to gene set enrichment analysis (GSEA) or Ingenuity Pathway
261 Analysis (IPA®, Ingenuity System, Redwood city, CA) software to reveal biological pathways
262 modulated by MIR17PTi.

263

264 **NOD SCID mice and *in vivo* model of human MM**

265 Male CB-17 severe combined immunodeficient (SCID) mice (6- to 8-weeks old; Harlan
266 Laboratories, Inc., Indianapolis) or female NOD/SCID- γ (NSG) mice (6- to 8-weeks old;
267 Charles River, Burlington, MA, USA) were housed and monitored in our Animal Research
268 Facility. All experimental procedures and protocols had been approved by the Institutional
269 Ethical Committee (Magna Graecia University) and conducted according to protocols
270 approved by the National Directorate of Veterinary Services (Italy). In accordance with
271 institutional guidelines, mice were sacrificed when tumors reached one or two cm in
272 diameter or in the event of paralysis or major compromise, to prevent unnecessary suffering.
273 NOD/SCID mice were s.c. inoculated with 5×10^6 NCI-H929 cells and treatments started
274 when palpable tumors became detectable, approximately 3 weeks following injection of MM
275 cells. NOD/SCID mice were also inoculated with 5×10^6 Luciferase gene-marked AMO1 (s.c.)
276 or AMO1/ABZB (s.c.). Treatments were i.v. performed. Tumors were measured by electronic
277 caliper and/or using IVIS LUMINA II Imaging System. The SCID-hu model was performed
278 as previously described by our group²⁹.

279
280 **Immunohistochemistry (IHC) and in situ hybridization (ISH)**

281 These experiments were performed as recently described by our group¹¹.

282

283 **Non-human primates study**

284 These experiments were performed as recently described by our group¹¹.

285

286 **Statistical Analysis**

287 All in vitro experiments were repeated at least three times and performed in triplicate; a
288 representative experiment was showed in figures. Statistical significances of differences
289 were determined using Student's t test, with minimal level of significance specified as
290 $P < 0.05$. Statistical significance of the in vivo growth inhibition was determined using
291 Student's t test. The minimal level of significance was specified as $P < 0.05$. All statistical
292 analyses were determined using GraphPad software (<http://www.graphpad.com>). Graphs
293 were obtained using GraphPad software.

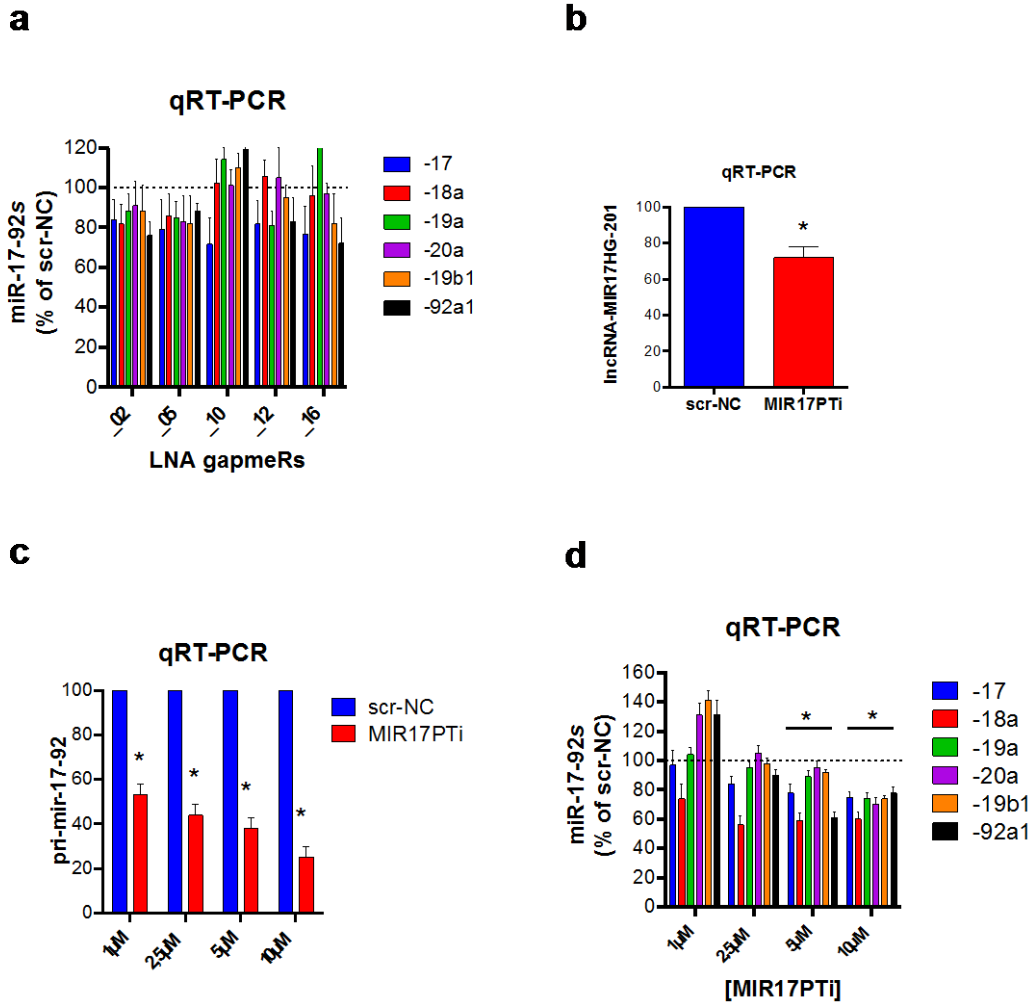
294

295 **Data availability**

296 The authors declare that all data supporting the findings of this study are available within
297 the article and its Supplementary Information Files or are available from the corresponding
298 authors on request.

Supplementary figures

Supplementary Figure 1



Supplementary Figure 1.

(a) qRT-PCR analysis of miR-17-92s expression in 293T two days after transfection with mir-17-92 LNA gapmeRs or scr-NC (25nM). The results are average expression levels after normalization with RNU44 and $\Delta\Delta C_t$ calculation (expressed as percentage of scr-NC).

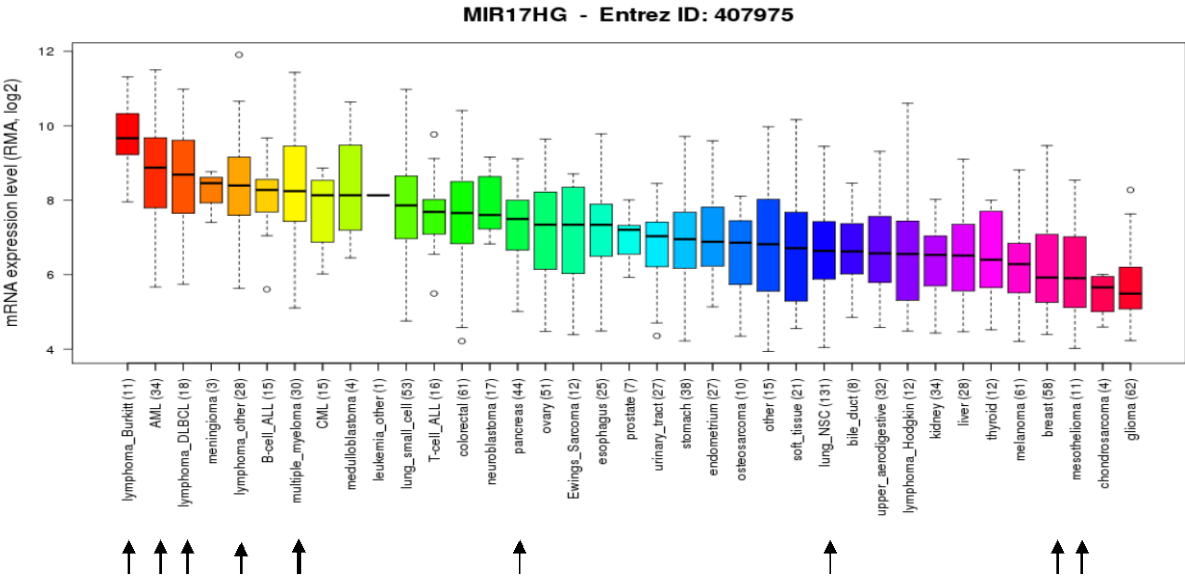
(b) qRT-PCR analyses of lncRNA MIR17HG-201 isoform in 293T two days after transfection with MIR17PTi or scr-NC (25nM). The results are average expression levels after normalization with GAPDH and $\Delta\Delta C_t$ calculation (expressed as percentage of scr-NC).

(c) qRT-PCR analysis of pri-mir-17-92 in 293T after six days of exposure to indicated concentrations of MIR17PTi or scr-NC. The results are average expression levels after normalization with GAPDH and $\Delta\Delta C_t$ calculations (expressed as percentage).

(d) qRT-PCR analysis of miR-17-92s in 293T after six days of exposure to indicated concentrations of MIR17PTi or scr-NC. The results are average expression levels after normalization with RNU44 and $\Delta\Delta C_t$ calculations (expressed as percentage).

Data from 1 out of 3 independent experiments is shown in each panel. * indicates $p < 0.05$

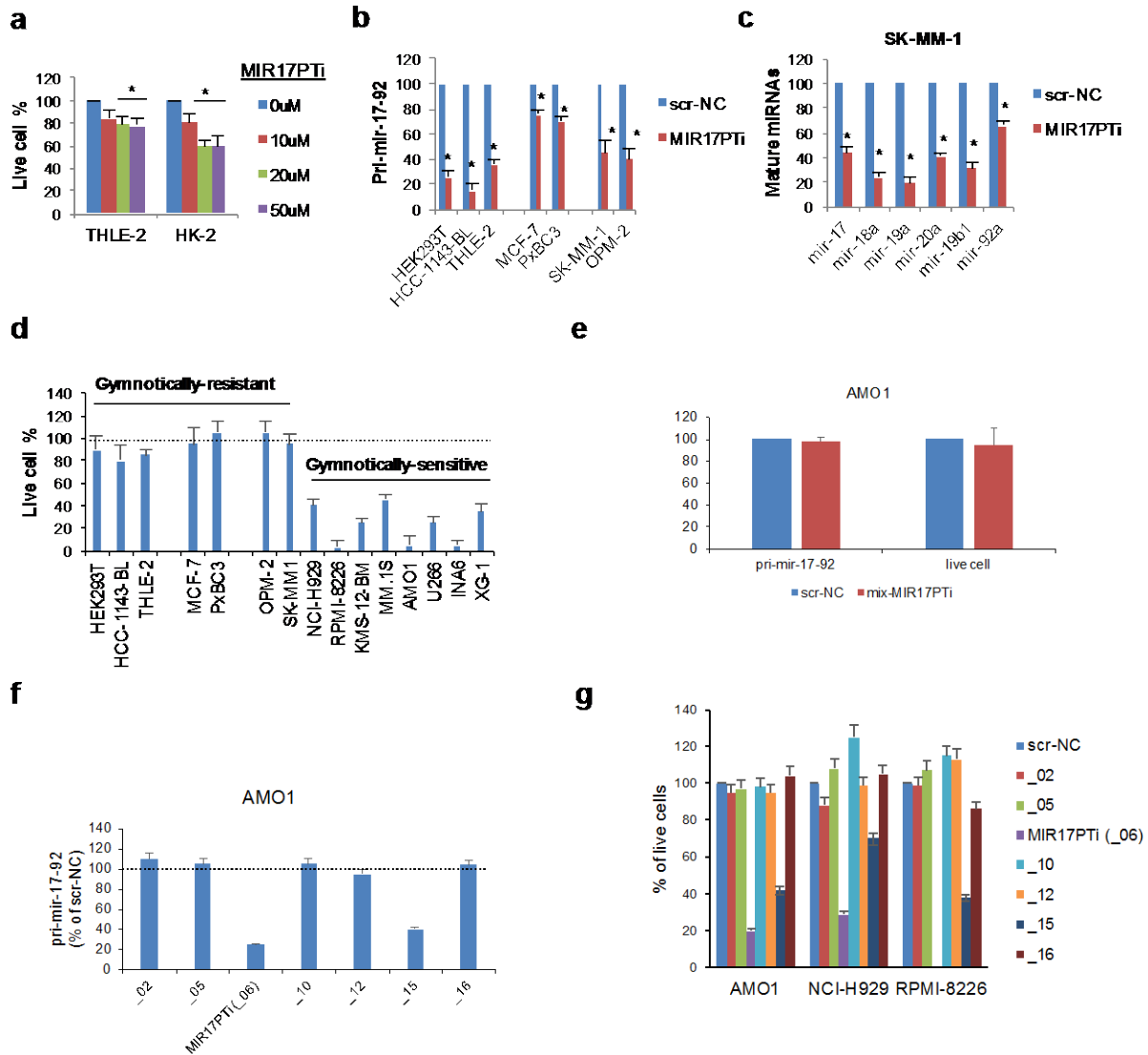
2



Supplementary Figure 2.

(a) MIR17HG expression at the CCLE. Arrows indicate CCLs used in Fig. 2a.

Supplementary Figure 3



Supplementary Figure 3.

(a) CCK-8 proliferation assay of two NM-CLs (THLE-2 and HK-2) exposed for six days to indicated concentrations of MIR17PTi.

(b) qRT-PCR analysis of pri-mir-17-92 in NM-CLs (n=3) and CCLs (n=4) exposed for six days to MIR17PTi (10μM) or equimolar scr-NC. Cell lines used in this panel were resistant to MIR17PTi (see Figure 2A and Supplementary Fig. S2A). The results shown are

average pri-mir-17-92 expression levels after normalization with GAPDH and $\Delta\Delta\text{Ct}$ calculation (expressed as percentage).

(c) qRT-PCR analysis of miR-17-92s expression in SK-MM1 exposed for six days to MIR17PTi (10 μ M) or equimolar scr-NC. The results are average expression levels after normalization with RNU44 and $\Delta\Delta\text{Ct}$ calculations (expressed as percentage).

(d) CCK-8 proliferation assay of NM-CLs (n=2) and CCLs (n=12) transfected with MIR17PTi (25nM) or equimolar scr-NC (two days after transfection).

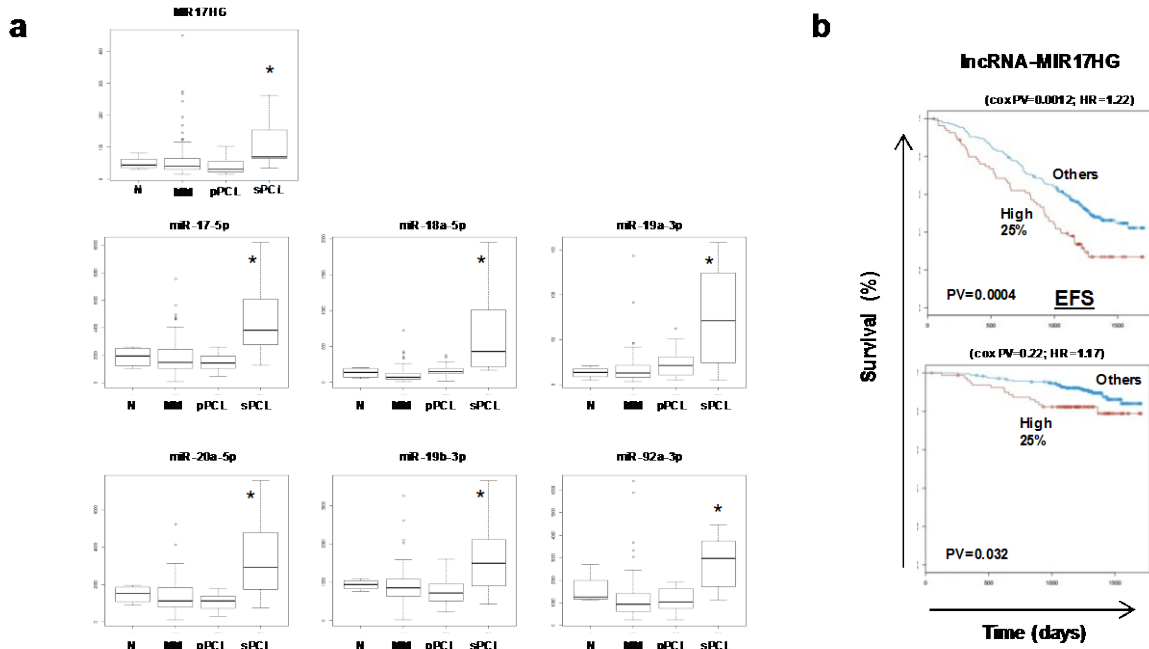
(e) Effects of mix-MIR17PTi on pri-mir-17-92 expression (left) and viability (right) after transfection of AMO1 cells (48h timepoint). The qRT-PCR results shown are average pri-mir-17-92 expression levels after normalization with GAPDH and $\Delta\Delta\text{Ct}$ calculation (expressed as percentage). Viability was measured by CCK-8 assay.

(f) qRT-PCR analysis of pri-mir-17-92 in AMO1 transfected with indicated miR-17-92 LNA gapmeRs (25nM) or equimolar scr-NC (two days after transfection).

(g) CCK-8 proliferation assay of AMO1 or NCI-H929 or RPMI-8226 transfected with indicated miR-17-92 LNA gapmeRs (25nM) or equimolar scr-NC (two days after transfection).

Data from 1 out of 3 independent experiments is shown in each panel. **indicates* $p < 0.05$

Supplementary Figure 4



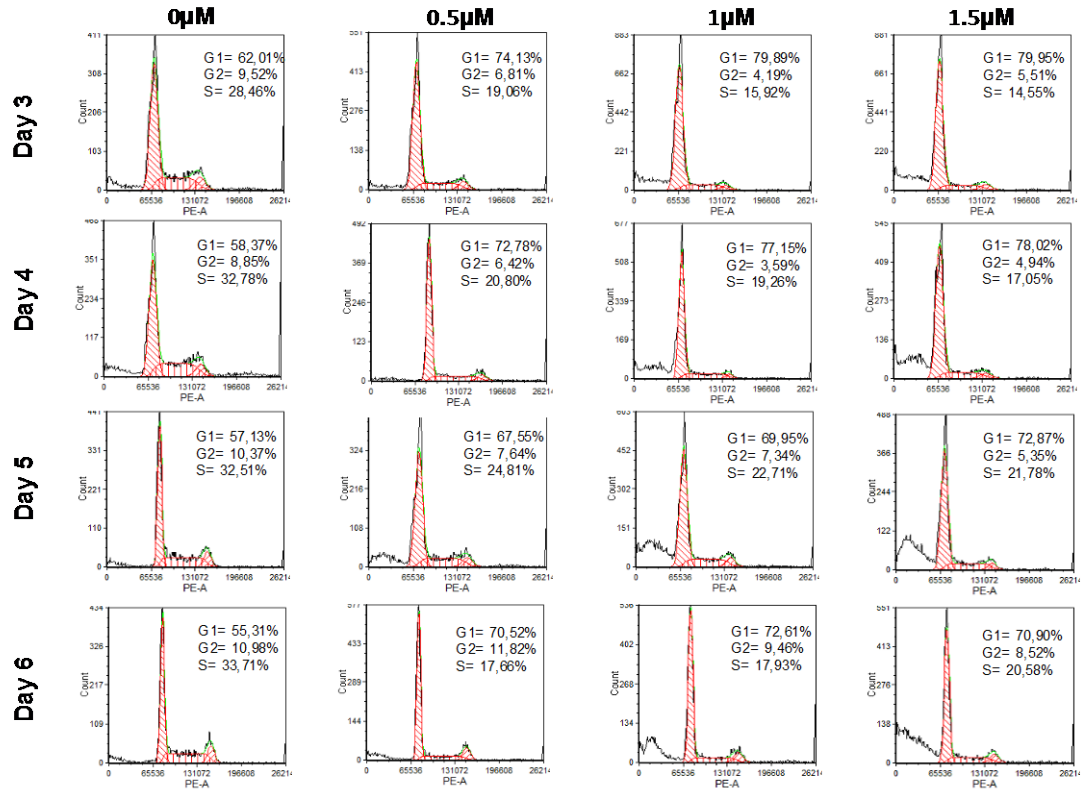
Supplementary Figure 4.

(a) Analysis of MIR17HG expression in CD138+ pMM cells (96 MM, 19 pPCL, 11 sPCL), as compared to normal donor-derived (N) CD138+ cells (n=4), from dataset series GSE70323 (GSE70319, MM; GSE73452, PCL) (upper panel); analysis of miR-17-92ss in CD138+ pMM cells (96 MM, 19 pPCL, 11 sPCL), as compared to normal donor-derived (N) CD138+ cells (n=4), from dataset series GSE70323 (GSE70254, MM; GSE73454, PCL).

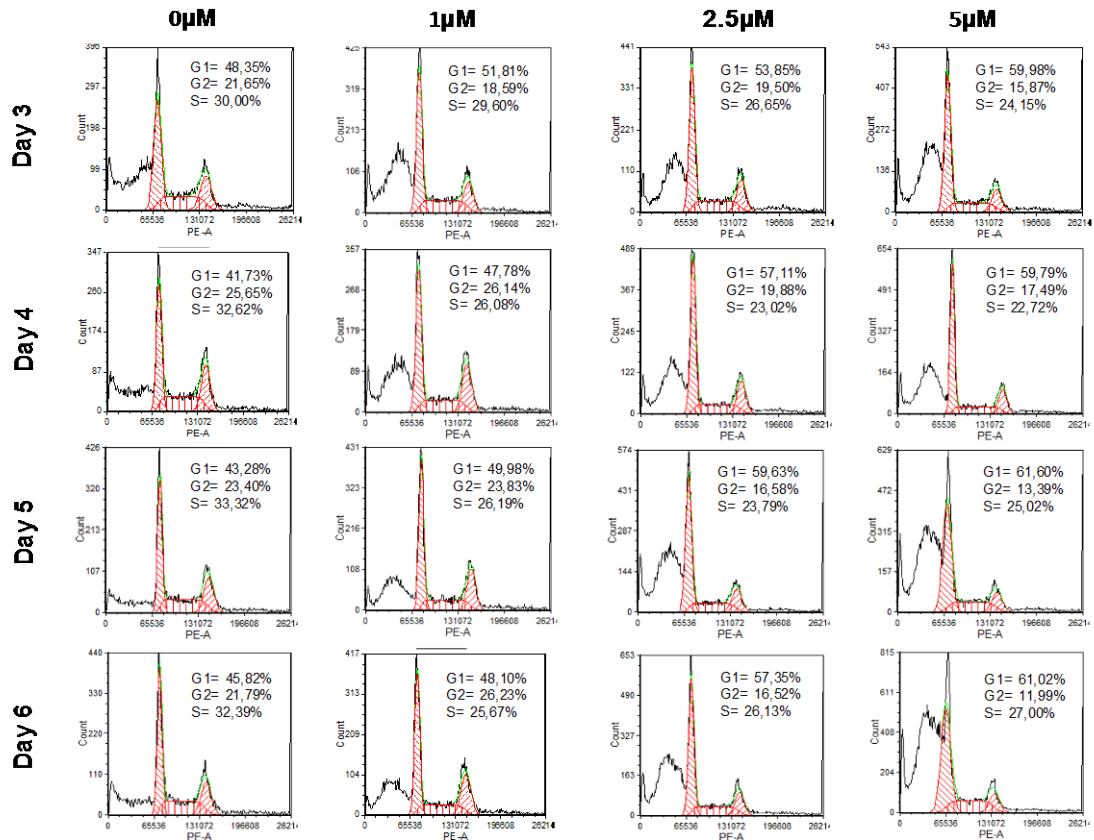
(b) RNA-seq analysis of the prognostic significance (PFS and OS) of pri-mir-17-92 expression in 320 newly-diagnosed MM patients from IFM/DFCI 2009 clinical study (NCT0191060).

Supplementary Figure 5

a



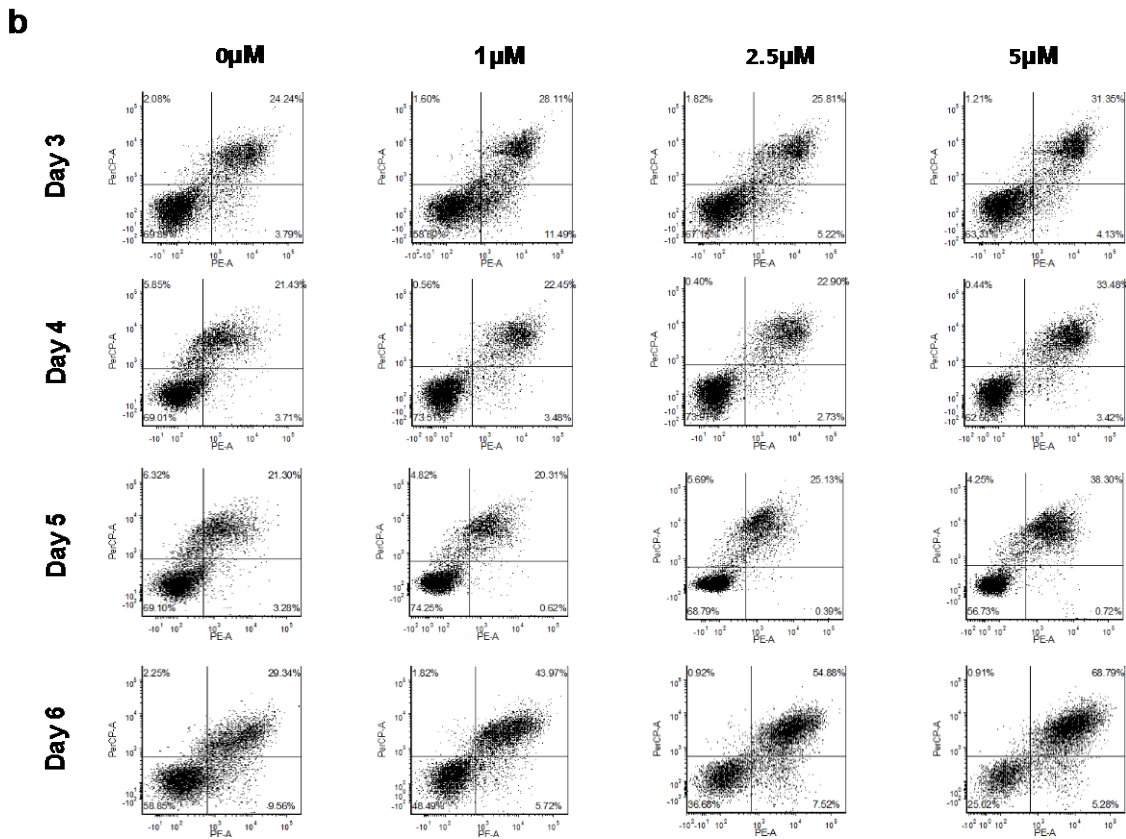
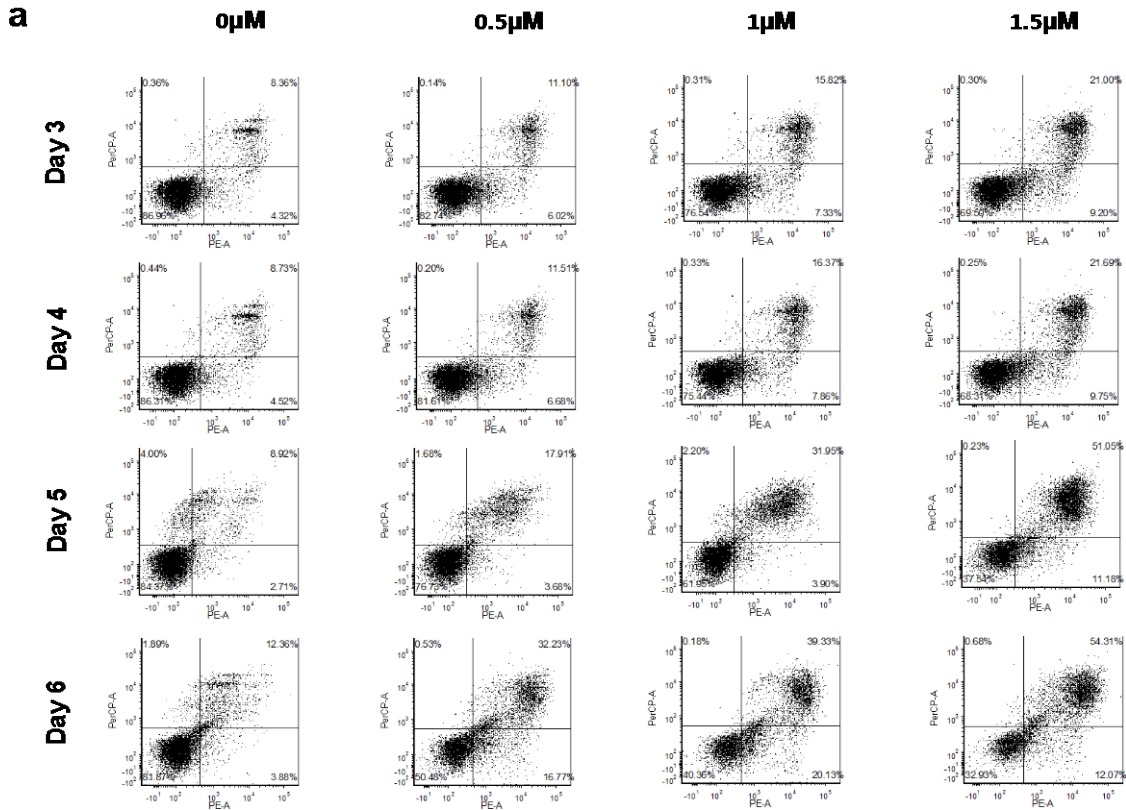
b



Supplementary Figure 5.

(a-b) Cell cycle analysis of (A) AMO1 and (B) NCI-H929 exposed for different days (3-4-5-6) to indicated concentrations of MIR17PTi.

Supplementary Figure 6

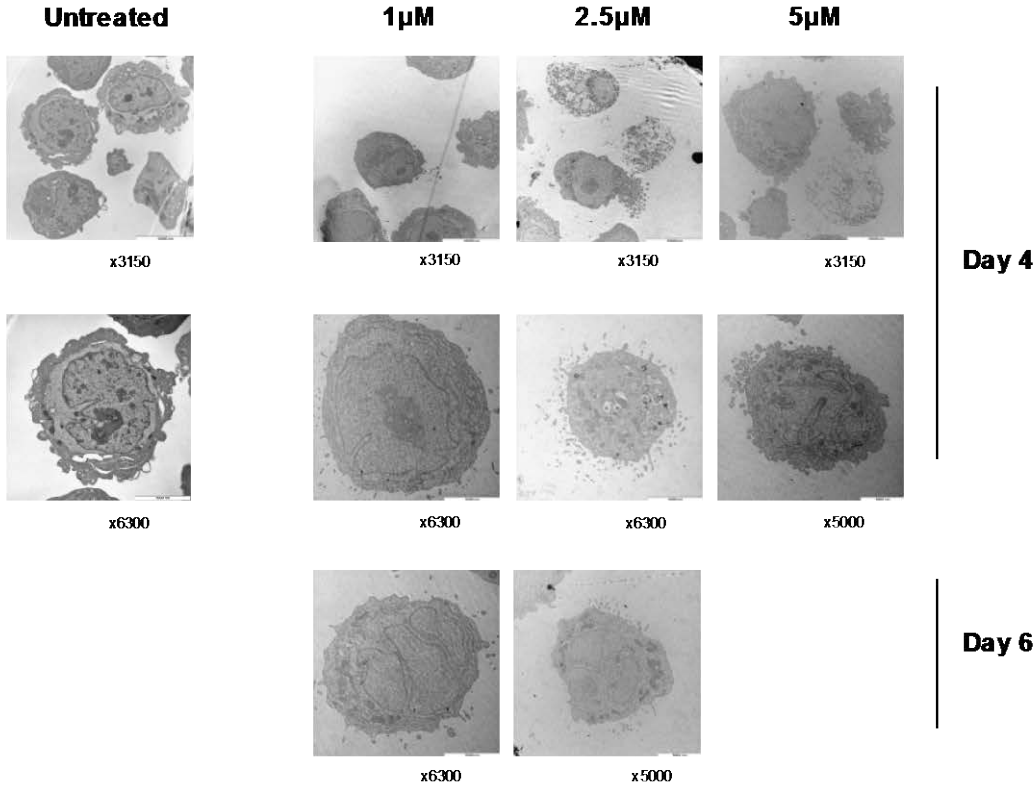


Supplementary Figure 6.

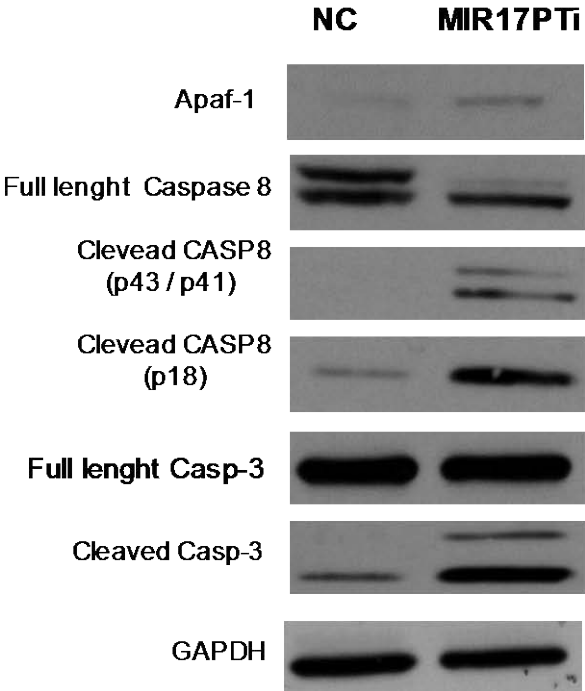
(a-b) Flow cytometry analysis of annexin V / 7-AAD stained (A) AMO1 and (B) NCI-H929 exposed for different days (3-4-5-6) to indicated concentrations of MIR17PTi.

Supplementary Figure 7

a



b



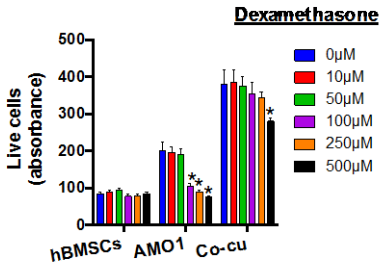
Supplementary Figure 7.

(a) Electron microscopy of NCI-H929 exposed for four or six days to indicated concentrations of MIR17PTi. Occurrence of apoptotic bodies is evident after treatment.

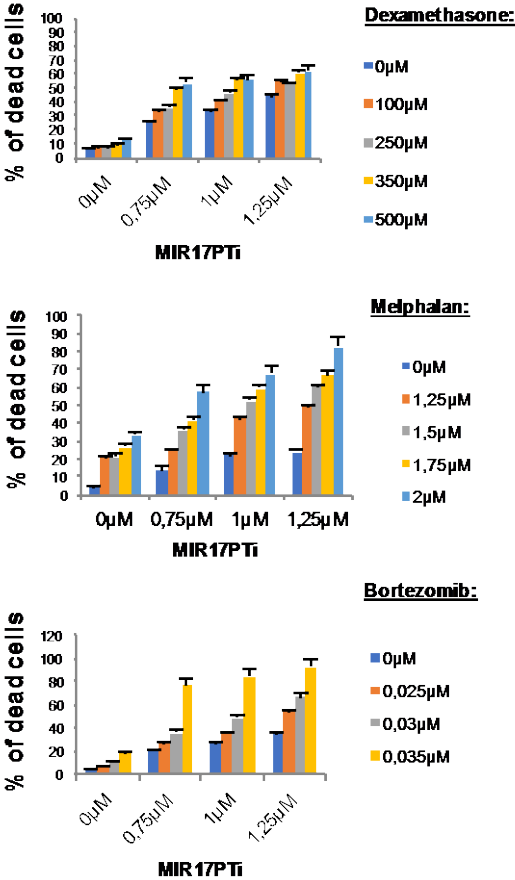
(b) Western blot analysis of apoptosis-related proteins in lysates from NCI-H929 exposed for six days to MIR17PTi (2.5 μ M) or scr-NC (2.5 μ M). GAPDH was used as protein loading control.

Supplementary Figure 8

a



b



Supplementary Figure 8.

(a) CCK-8 assay of hBMSCs, AMO1 or AMO1 co-cultured with hBMSCs after six days of exposure to indicated concentrations of dexamethasone.

(b) Flow-cytometry analysis of 7-AAD stained AMO1 after six days of treatment with MIR17PTi (0-0.75-1-1.25 μM) and indicated concentrations of dexamethasone, melphalan or bortezomib. Data from 1 out of 3 independent experiments is shown in each panel.

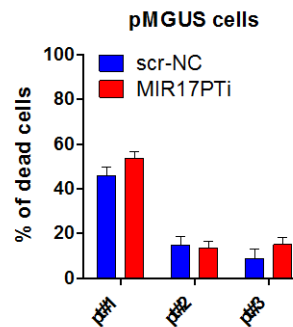
Data from 1 out of 3 independent experiments is shown in each panel. *indicates $p < 0.05$

Supplementary Figure 9

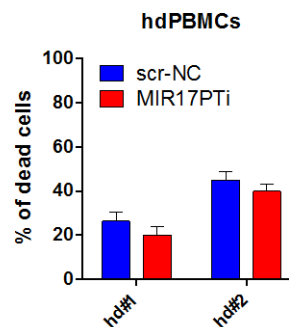
a

PATIENT ID	% of CD138+	Stage
MM#1	99	IM / ND
MM#2	70	IM / ND
MM#3	94	IM / ND
MM#4	98.5	IM / ND
MM#5	93	IM / Rel
MM#6	97	IM / ND
MM#7	90	IM / ND
MM#8	97	IM / ND
MM#9	98.1	IM / ND
MM#10	99.8	IM / Rel
MM#11	99.7	IM / ND
MM#12	95	EM / Rel
MM#13	95	EM / Rel
MGUS#1	77	IM
MGUS#2	52	IM
MGUS#3	60	IM

b



c



Supplementary figure 9.

(a) Table showing the purity (% of CD138+ cells) and clinical stage (IM: intra-medullary disease; EM: extra-medullary disease; ND: newly diagnosis; Rel: relapsed disease) of immunoselected cells from MM or MGUS patients.

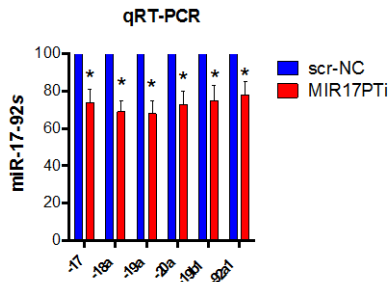
(b) Flow-cytometry analysis of 7-AAD stained CD138+ MGUS cells exposed for six days to MIR17PTi or scr-NC (2,5µM).

(c) Flow-cytometry analysis of 7-AAD stained healthy donor-PBMCs exposed for six days to MIR17PTi or scr-NC (10µM).

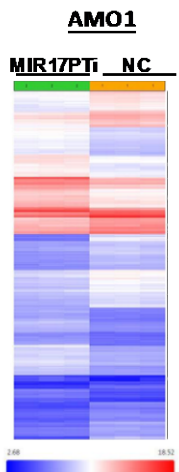
*indicates $p < 0.05$

Supplementary Figure 10

a



b



c



d

Dataset	Size	NES	FDR q-val
SCHUMACHER_MYC_TARGETS_UP	74	2.27	0.04
DANG_MYC_TARGETS_UP	120	2.25	0.04
MENSEN_MYC_TARGETS	48	2.15	0.04
DANG_REGULATED_BY_MYC_UP	66	1.69	0.06

Supplementary Figure 10.

(a) qRT-PCR analysis of miR-17-92s in pMM cells (n=3) exposed for six days to MIR17PTi (2,5 μ M) or equimolar scr-NC. The results shown are average miR-17-92s expression levels after normalization with RNU44 and $\Delta\Delta$ Ct calculation (expressed as percentage).

(b) Hierarchical clustering of AMO1 exposed for six days to MIR17PTi (1 μ M) or equimolar scr-NC.

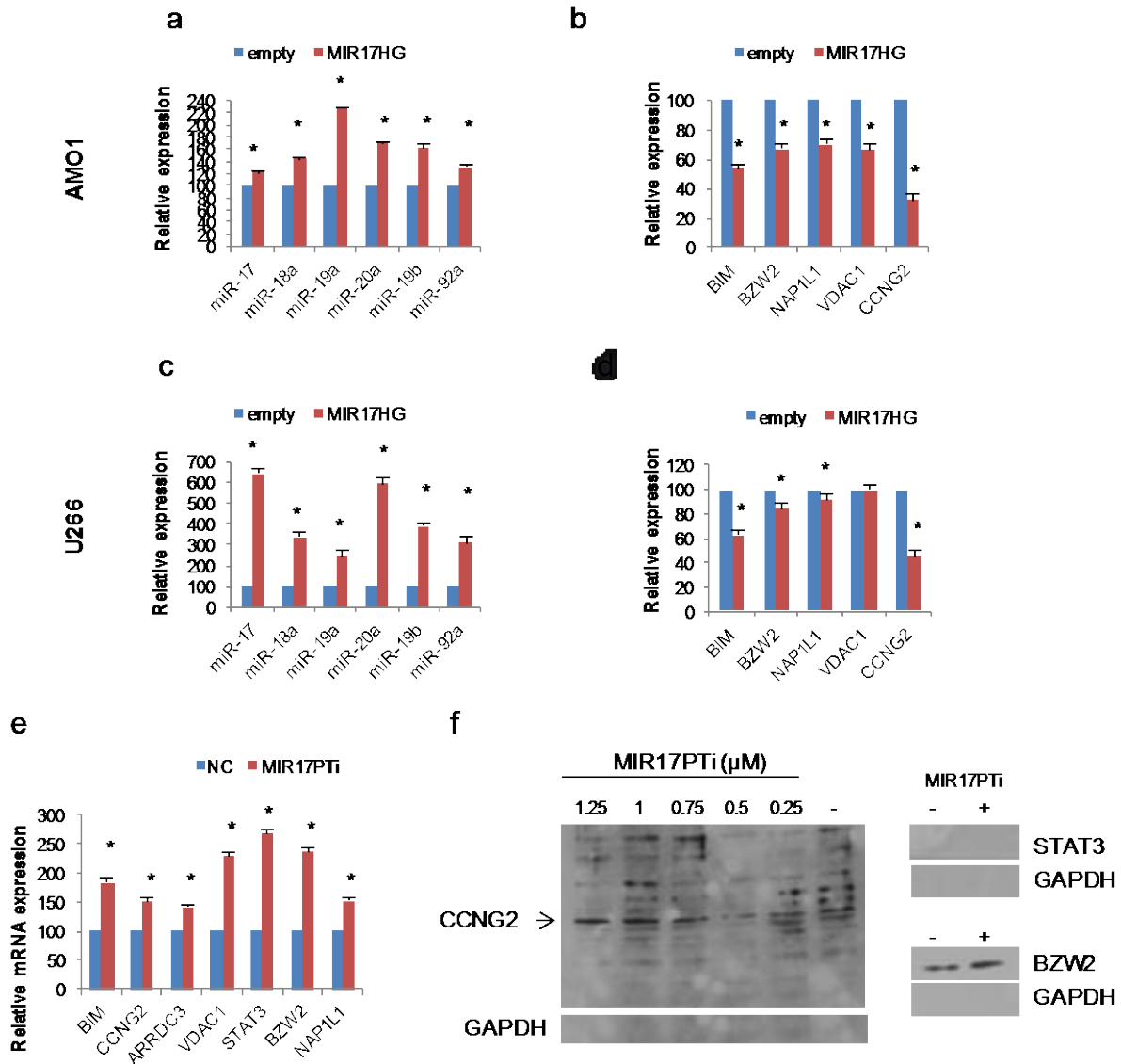
(c) Enrichment plot of the HALLMARK_MYC_TARGET_V1 in the positive phenotype (relative to AMO1 exposed to MIR17PTi).

(d) Table of gene sets, from the Hallmark collection, enriched of genes upregulated by MIR17PTi (positive phenotype) in AMO1 exposed to MIR17PTi (1 μ M) for six days.

Number of genes in each set (size), the normalized enrichment score (NES), and test of statistical significance (FDR q value) are highlighted.

**indicates $p < 0.05$*

Supplementary Figure 11



Supplementary Figure 11.

(a-b) qRT-PCR analysis of (A) miR-17-92s and (B) indicated mRNAs in AMO1 transduced with a miR-17-92s lentiviral vector.

(c-d) qRT-PCR analysis of (C) miR-17-92s and (D) indicated mRNAs in U266 transduced with a miR-17-92s lentiviral vector.

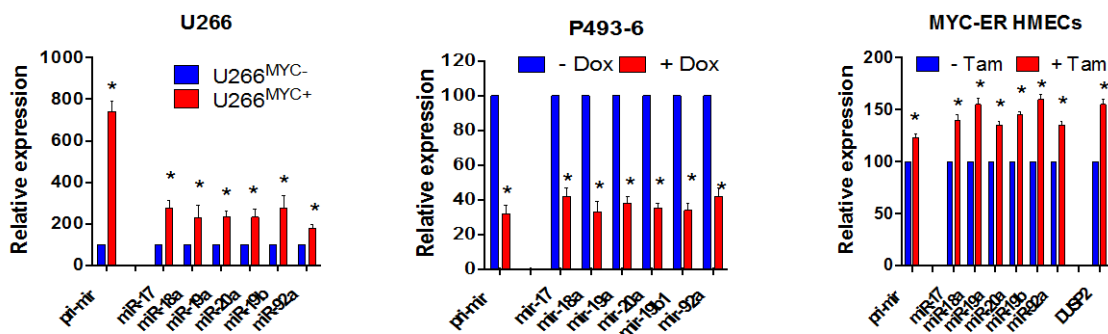
(e) qRT-PCR analysis of indicated mRNAs in AMO1 exposed to MIR17PTi (1 μ M) for six days. The results shown are average miRNA or mRNA expression levels after normalization with RNU44 or GAPDH and $\Delta\Delta$ Ct calculation (expressed as percentage).

(f) Western blot analysis of CCNG2, BZW2 and STAT3 in lysates from AMO1 exposed to MIR17PTi for six days. GAPDH was used as protein loading control.

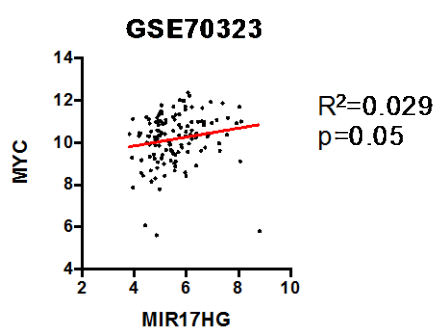
**indicates $p < 0.05$*

Supplementary Figure 12

a



b



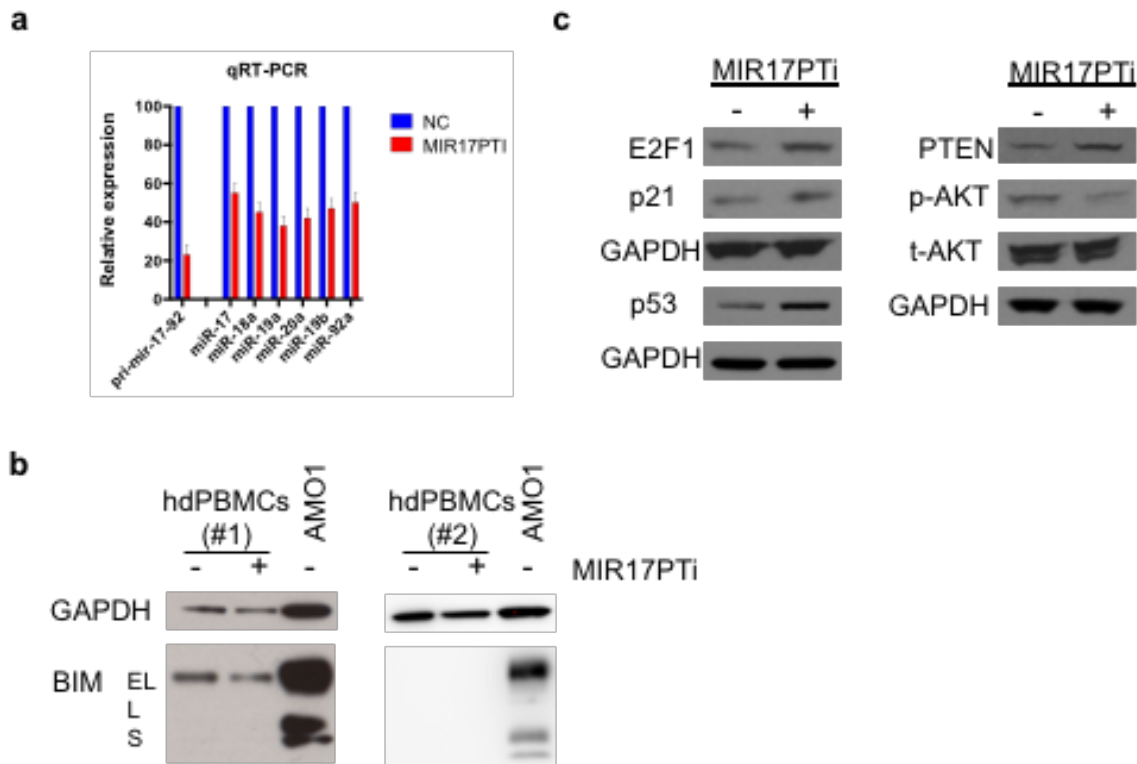
Supplementary Figure 12.

(a) qRT-PCR analysis of pri-mir-17-92 and miR-17-92s in: (left panel) U266^{MYC+} as compared to U266^{MYC-}; P493-6 cultured for two days with or without doxycycline (Dox); MYC-ER HMECs cultured for two days with or without tamoxifen (Tam). In this latter panel it is also shown the expression of DUSP2 as positive control of MYC activation. The results shown are average pri-mir-17-92 or DUSP2 or miR-17-92s expression levels after normalization with GAPDH (pri-mir-17-92 and DUSP2) or RNU44 (miR-17-92s), and $\Delta\Delta Ct$ calculations (expressed as percentage).

(b) Integrative analysis of MYC and MIR17HG in CD138+ pMM cells (96 MM, 19 pPCL, 11 sPCL) from dataset series GSE70323 (GSE70319, MM; GSE73452, PCL).

Data from 1 out of 3 independent experiments is shown in each panel. * indicates $p < 0.05$

Supplementary Figure S13



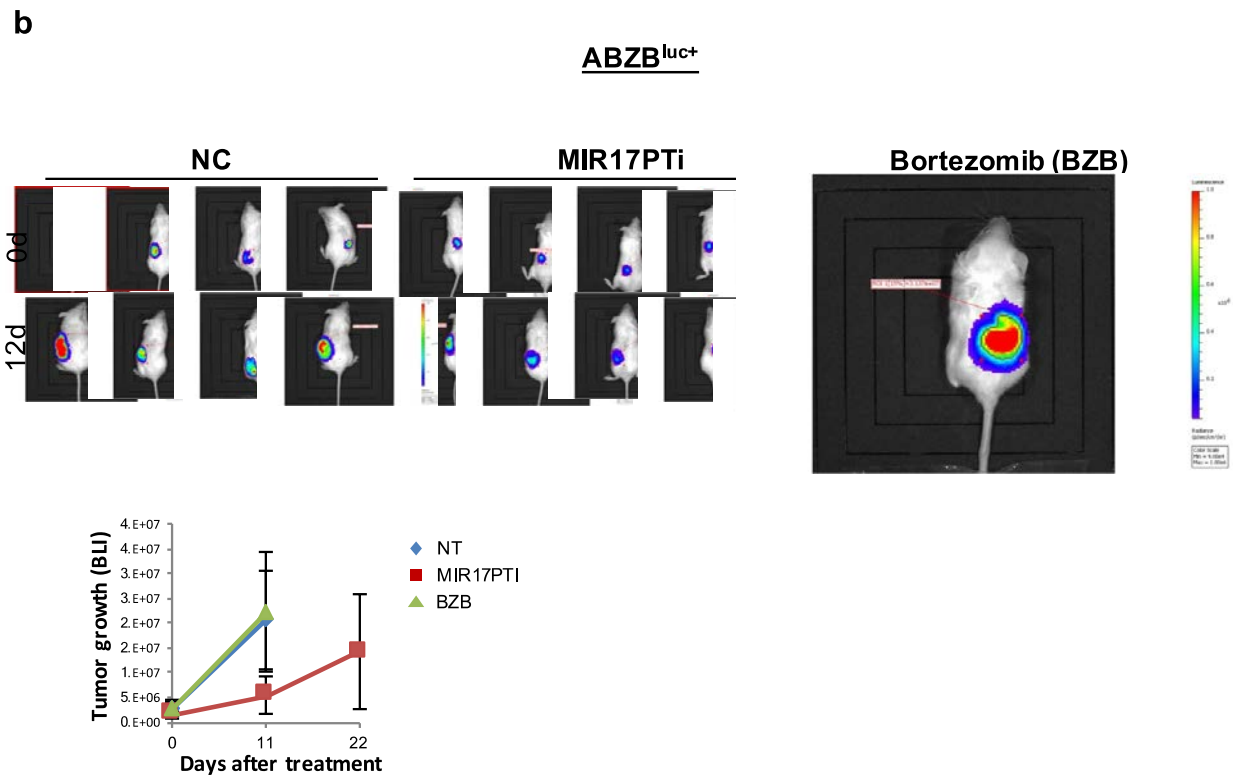
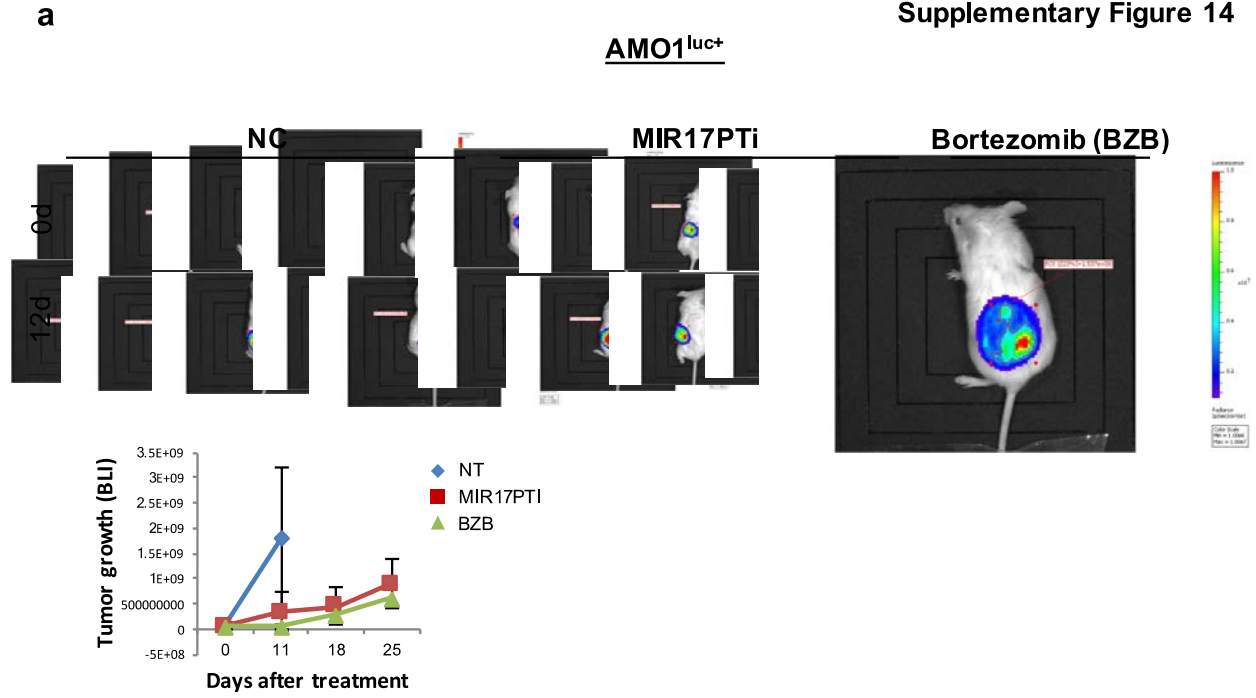
Supplementary Figure S13.

(a) qRT-PCR analysis of pri-mir-17-92 and miR-17-92s in healthy donor PBMCs (hdPBMCs; n=2) after 6 days of treatment with MIR17PTi (5 μM) or equimolar scr-NC. The results shown are average pri-mir-17-92 or miR-17-92s expression levels after normalization with GAPDH (pri-mir-17-92) or RNU44 (miR-17-92s), and $\Delta\Delta C_t$ calculations (expressed as percentage).

(b) Western blot analysis of BIM in lysates from hdPBMCs (n=2) after 6 days of treatment with MIR17PTi or scr-NC 5 μM or AMO1 (basal level). GAPDH was used as protein loading control.

(c) Western blot analysis of E2F1, p21, P53, PTEN, p-AKT and t-AKT in lysates from NCI-H929 exposed to MIR17PTi (2.5 μM) for six days. GAPDH was used as protein loading control.

Supplementary Figure 14

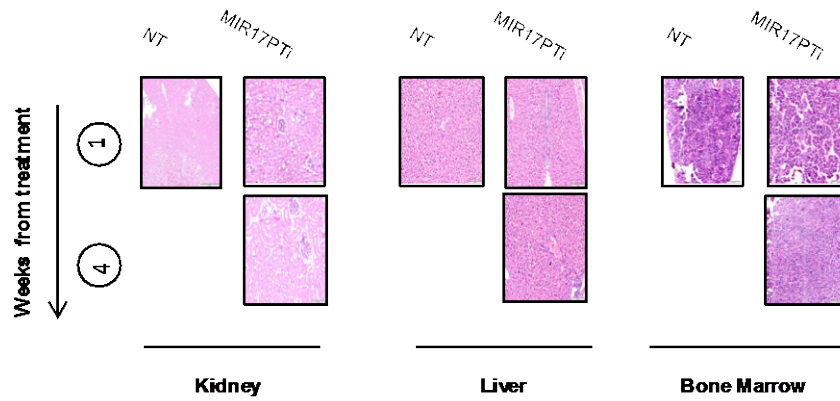


Supplementary Figure 14.

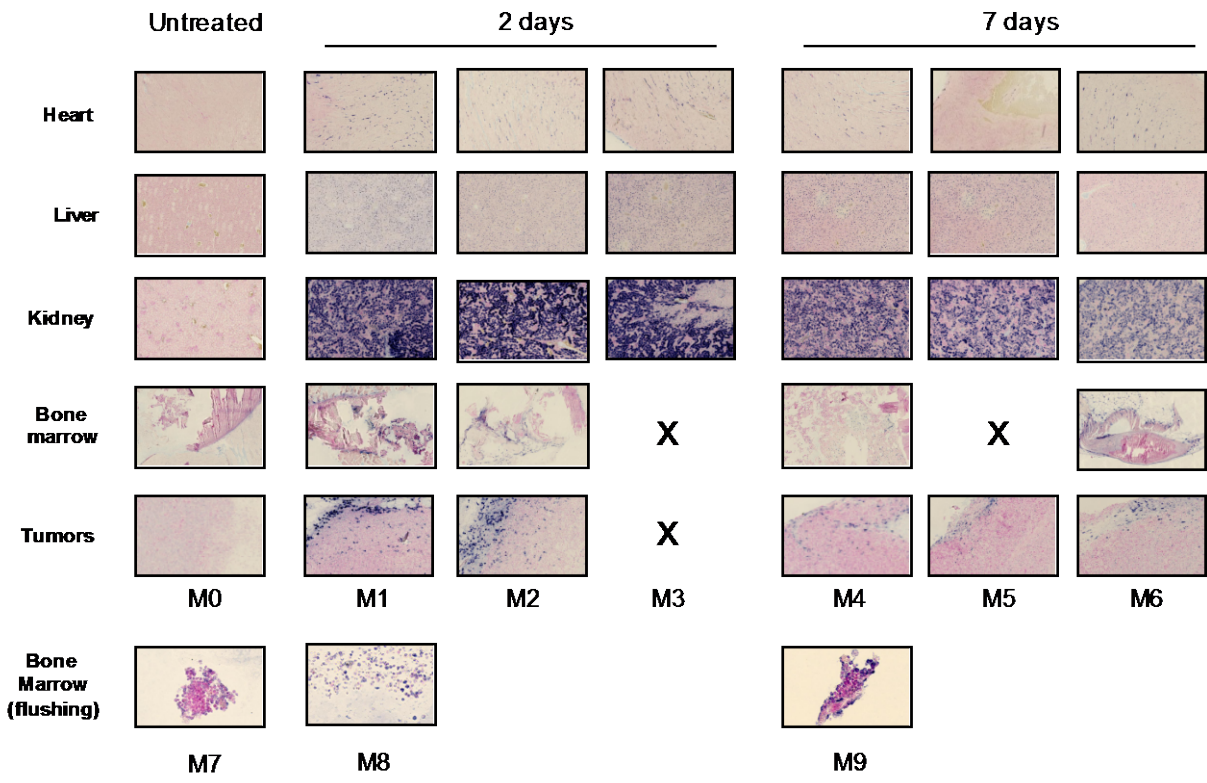
(a-b) IVIS images of NOD SCID mice s.c. xenografted with luciferase gene-marked (A) AMO1 or (B) ABZB. Tumor growth, as assessed by BLI analysis, is also reported.

Supplementary Figure 15

a



b



Supplementary Figure 15.

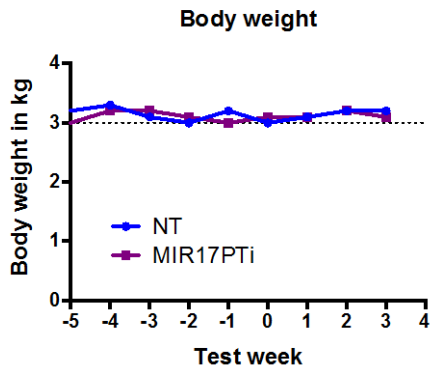
(a) H&E staining of kidney, liver and bone marrow from mice i.v. injected with MIR17PTi (2mg/kg) at days 1-4-8-15-22. Mice were sacrificed one or four weeks after last injection.

(b) Detection of MIR17PTi by ISH analysis of indicated organs or NCI-H929 retrieved xenografts (tumors). Mice were sacrificed two or seven days after single dose of MIR17PTi 2mg/kg.

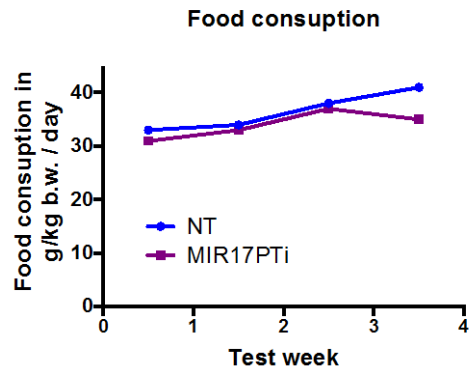
Organs and tumor from untreated mouse is also shown.

Supplementary Figure 16

a



b

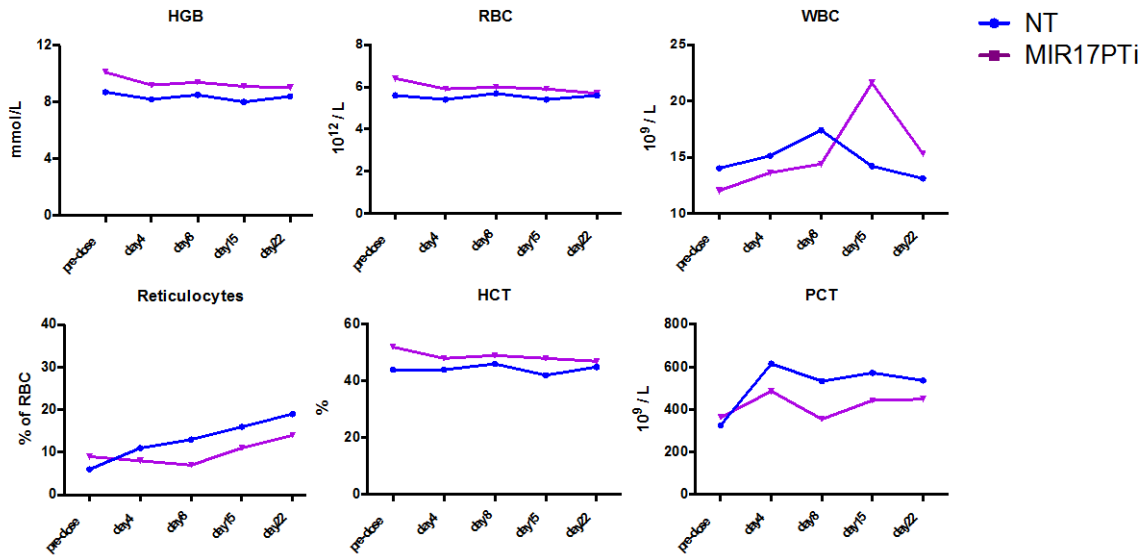


Supplementary Figure 16.

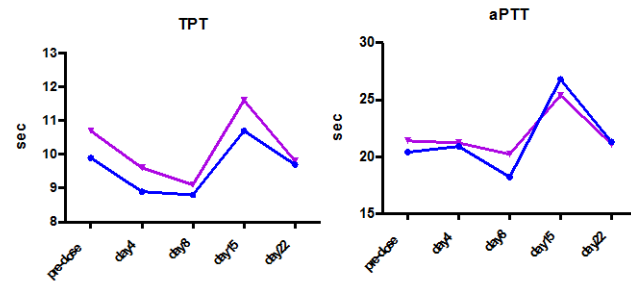
(a) Body weight and (b) food consumption of Cynomolgus monkeys (n=2) i.v. injected with MIR17PTi (0.504mg/kg) or saline solution at days 1-4-8-15-22. Both parameters were evaluated once weekly for four weeks after first injection.

Supplementary Figure 17

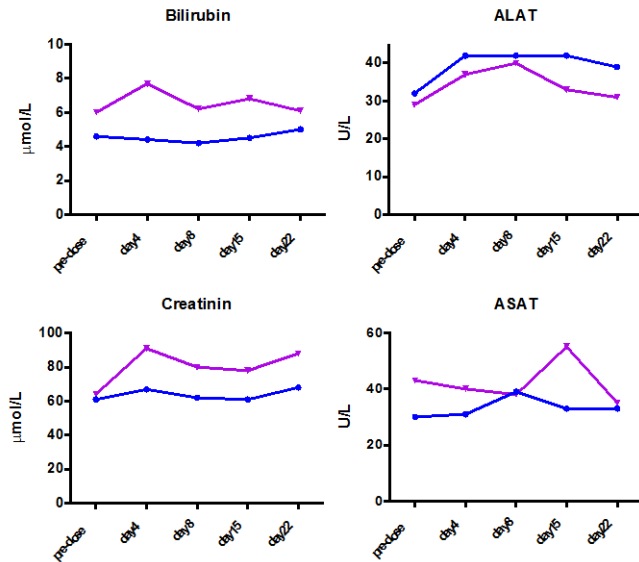
a



b



c



Supplementary Figure 17.

(a) Hematology, **(b)** coagulation and **(c)** clinical biochemistry parameters in Cynomolgus monkeys (n=2) i.v. injected with MIR17PTi (0.504mg/kg) or saline solution at days 1-4-8-15-22. Sampling was performed before treatment (pre-dose) and at days 4-8-15 and 22.

Supplementary Table

Supplementary Table S1. miR-17-92s targets upregulated by MIR17PTi in sensitive pMM cells.

Gene symbol	Gene Family (according to IPA)	Targeting miRNA (predicted by miRcode)	Targeting miRNAs (validated by 3'UTR luciferase assay)	MYC-binding loci	MYC direct targeting	MYC direct targeting (validated in B cells)	Upregulated in AMO1 by MIR17PTi (p<0.05)	Upregulated in resistant pMM cells by MIR17PTi
AGPAT5	Enzyme	-19 / -25						
AKAP13	Other	-17 / -18 / -19 / -25		V ²¹	V (neg) ²¹	V ²¹		
ANKRD28	Other	-17 / -18 / -19 / -25						
ATOX1	Transporter	-17 / -18 / -19 / -25		V ⁴⁰				
ATP2B1	Transporter	-17 / -18 / -19 / -25						
BCL2L11	Other	-17 / -19 / -25	V ⁴¹	V ¹⁷	V (pos) ^{17,26}	V ¹⁷	V	
BICD2	Other	-17 / -19 / -25		V ²¹	V (pos) ²¹	V ²¹	V	
BTG2	Transcription Regulator	-17 / -18 / -25						
BZW2	Translation regulator	-17 / -19		V ^{20,21}	V (pos) ^{20,21}	V ^{20,21}	V	
CDK13	Kinase	-17 / -18 / -19						
CHD4	Enzyme	-17					V	
COL4A3BP	Kinase	-25						
DDX42	Enzyme	-18						
DDX6	Enzyme	-17 / -19 / -25		V ²¹				
DUSP2	Phosphatase	-17		V ²¹	V (pos) ²¹			
ESYT1	Other	-19						
GNAS	Enzyme	-17 / -18 / -19 / -25		V ²¹	V (neg) ²¹	V ²¹		
GRK6	Kinase	-19						
H2AFV	Other	-17 / -18		V ²¹				
HECA	Other	-17						
HP1BP3	Other	-17 / -18 / -25						
IGF2R	Transmembrane Receptor	-18 / -19 / -25						
ILF3	Transcription Regulator	-19 / -25						
IPO7	Transporter	-17 / -25		V ²¹	V (pos) ²¹	V ²¹		
KIAA0226	Other	-17 / -18		V ²¹				
KIAA1432	Other	-17 / -18 / -19 / -25						
MAML1	Transcription Regulator	-18 / -19 / -25						
MAN2A1	Enzyme	-17 / -19 / -25		V ²¹			V	
MAT2A	Enzyme	-17 / -19		V ¹⁹	V (pos) ¹⁹	V ¹⁹		
MBOAT2	Enzyme	-17 / -19 / -25					V	
MBTPS1	Peptidase	-17		V ²¹				
MLXIP	Other	-17 / -25		V ⁴²	V (pos) ⁴²		V	
NAP1L1	Other	-18 / -19 / -25		V ²⁰	V (pos) ²⁰	V ²⁰	V	V

Gene symbol	Gene Family (according to IPA)	Targeting miRNAs (predicted by miRcode)	Targeting miRNAs (validated by 3' UTR luciferase assay)	MYC-binding loci	MYC direct targeting	MYC direct targeting (validated in B cells)	Upregulated in AMO1 by MIR17PTi	Upregulated in resistant pMM cells by MIR17PTi
NPTN	Other	-19 / -25						
NR4A2	Ligand Dependent Nuclear Receptor	-17 / -19						
OTUD1	Peptidase	-17 / -19						
PARP8	Other	-18 / -19 / -25					V	
PFN1	Other	-19 / -25		V ²¹				
PHF1	Transcription regulator	-17 / -25						
PNRC1	Other	-19						
PTK2B	Kinase	-17 / -18 / -19		V ²¹	V (neg) ²¹	V ²¹	V	
RAB30	Enzyme	-17 / -19 / -25						
RAF1	Kinase	-17 / -19						
RASSF3	Other	-17 / -18 / -19 / -25		V ²¹				
RBM3	Other	-18						
RNF145	Other	-17 / -18 / -19					V	
SKIL	Transcription Regulator	-17 / -19 / -25		V ²¹	V (neg) ²¹	V ²¹		
SLC31A2	Transporter	-17 / -18 / -19						
SLC5A6	Transporter	-17 / -19		V ¹⁹	V (pos) ¹⁹	V ¹⁹		
SSFA2	Other	-17 / -18 / -25						
SYPL1	NA	-18 / -19 / -25						
TCEB3	Transcription regulator	-17 / -19 / -25		V ¹⁹				
TGFBR2	Kinase	-17 / -19 / -25	V ⁴³					
TNPO2	Transporter	-19		V ²¹				
TRAM2	Other	-17 / -18 / -25					V	
TRIM8	Other	-17 / -18		V ²¹	V (neg) ²¹	V ²¹		
UBFD1	Other	-17 / -19		V ⁴⁴				
UBQLN4	Other	-17						
USP21	Peptidase	-18 / -19 / -25						
VDAC1	Ion channel	-17		V ²¹	V (pos) ²¹	V ²¹	V	
VPS52	Other	-18						
WNK3	Kinase	-17 / -18 / -19		V ²¹				
YAF2	Transcription regulator	-17 / -18 / -19		V ²¹				
ZC3H7B	Other	-17 / -18						
ZDHHC18	NA	-19						

Supplementary References

1. Zeller KI, Zhao X, Lee CW, et al. Global mapping of c-Myc binding sites and target gene networks in human B cells. Proc Natl Acad Sci U S A. 2006;103(47):17834-17839.

2. Sertel S, Eichhorn T, Simon CH, Plinkert PK, Johnson SW, Efferth T. Pharmacogenomic identification of c-Myc/Max-regulated genes associated with cytotoxicity of artesunate towards human colon, ovarian and lung cancer cell lines. *Molecules*. 2010;15(4):2886-2910.
3. Xiao C, Srinivasan L, Calado DP, et al. Lymphoproliferative disease and autoimmunity in mice with increased miR-17-92 expression in lymphocytes. *Nat Immunol*. 2008;9(4):405-414.
4. Egle A, Harris AW, Bouillet P, Cory S. Bim is a suppressor of Myc-induced mouse B cell leukemia. *Proc Natl Acad Sci U S A*. 2004;101(16):6164-6169.
5. Muthalagu N, Junttila MR, Wiese KE, et al. BIM is the primary mediator of MYC-induced apoptosis in multiple solid tissues. *Cell Rep*. 2014;8(5):1347-1353.
6. Wu CH, Sahoo D, Arvanitis C, Bradon N, Dill DL, Felsher DW. Combined analysis of murine and human microarrays and ChIP analysis reveals genes associated with the ability of MYC to maintain tumorigenesis. *PLoS Genet*. 2008;4(6):e1000090.
7. Li Z, Van Calcar S, Qu C, Cavenee WK, Zhang MQ, Ren B. A global transcriptional regulatory role for c-Myc in Burkitt's lymphoma cells. *Proc Natl Acad Sci U S A*. 2003;100(14):8164-8169.
8. Carroll PA, Diolaiti D, McFerrin L, et al. Deregulated Myc requires MondoA/Mlx for metabolic reprogramming and tumorigenesis. *Cancer Cell*. 2015;27(2):271-285.
9. Li L, Shi JY, Zhu GQ, Shi B. MiR-17-92 cluster regulates cell proliferation and collagen synthesis by targeting TGFB pathway in mouse palatal mesenchymal cells. *J Cell Biochem*. 2012;113(4):1235-1244.
10. Sabo A, Kress TR, Pelizzola M, et al. Selective transcriptional regulation by Myc in cellular growth control and lymphomagenesis. *Nature*. 2014;511(7510):488-492.